A SIMPLE DIFFUSE INTERFACE METHOD FOR THE SIMULATION OF COMPLEX FREE-SURFACE FLOWS

Michael Dumbser

[1]Department of Civil and Environmental Engineering, University of Trento, Italy, Via Mesiano, 77, I-38123 Trento
E-mail: michael.dumbser@unitn.it

Abstract

In this article we propose a simple and efficient diffuse interface (interface–capturing) two–phase algorithm for the simulation of complex non–hydrostatic free surface flows in general geometries [1]. The physical model is given by a special case of the more general Baer–Nunziato model for compressible multi–phase flows. In the applications considered here, the relative pressure of the gas phase with respect to atmospheric reference conditions is assumed to be zero everywhere and the momentum of the gas phase can be neglected compared to the one of the liquid. The reduced system is closed by the Tait equation of state, which is a widespread model for water. The resulting PDE system is solved by a high order path–conservative WENO finite volume scheme on unstructured triangular meshes, to be applicable also in complex geometries. To assure low numerical dissipation at the free surface, which actually is crucial for the applications under consideration here, we use the new generalized Osher–type scheme of Dumbser and Toro [2], which resolves steady shear and contact waves exactly, in contrast to the simpler centered path–conservative FORCE schemes presented in [3]. The model derives directly from first principles, namely the conservation of mass and momentum, hence it does not make any of the classical simplifications inherent in the commonly used shallow water models, which are based on depth-averaging, neglecting accelerations in gravity directions and on the resulting hydrostatic pressure distribution. We validate the new two–phase model against available analytical, numerical and experimental reference solutions and we also show some comparisons with the classical shallow water model for typical dambreak–type problems.

Introduction

Most state of the art free surface flow models commonly used in environmental engineering and geophysics are based on some kind of depth–averaged shallow water type flow model. The most basic two–dimensional shallow water model with fixed bed, without friction and with only one single layer of liquid is given by the following nonlinear PDE system:

$$\begin{aligned} &\frac{\partial h}{\partial t} + \nabla \cdot h\boldsymbol{v} = 0 \\ &\frac{\partial h\boldsymbol{v}}{\partial t} + \nabla \cdot \left(h\boldsymbol{v}\boldsymbol{v} + \frac{1}{2} g h^2 \boldsymbol{I}\right) = -gh\nabla b \end{aligned} \tag{1}$$

Here, h denotes the total water depth, $\boldsymbol{v}$ is the velocity vector, $b = b(x)$ is the known, fixed, bottom elevation, $\boldsymbol{I}$ is the identity matrix and g is the gravity acceleration. The location of the free surface is given by the above model as $\eta = h + b$.

The Full Baer-Nunziato Model of Compressible Multi-Phase Flows

The original Baer–Nunziato system [4] with gravity effects reads for a mixture of two inviscid fluids as

$$\begin{aligned} &\frac{\partial \alpha_1\rho_1}{\partial t} + \nabla \cdot \alpha_1\rho_1\boldsymbol{v_1} = 0 \\ &\frac{\partial \alpha_1\rho_1\boldsymbol{v_1}}{\partial t} + \nabla \cdot (\alpha_1(\rho_1\boldsymbol{v_1}\boldsymbol{v_1} + p_1\boldsymbol{I})) = p_I\nabla\alpha_1 + \alpha_1\rho_1 g \\ &\frac{\partial \alpha_1\rho_1 E_1}{\partial t} + \nabla \cdot \left(\alpha_1\boldsymbol{v_1}(\rho_1 E_1 + p_1)\right) = -p_I \frac{\partial}{\partial t}\alpha_1 \\ &\frac{\partial \alpha_2\rho_2}{\partial t} + \nabla \cdot \alpha_2\rho_2\boldsymbol{v_2} = 0 \\ &\frac{\partial \alpha_2\rho_2\boldsymbol{v_2}}{\partial t} + \nabla \cdot (\alpha_2(\rho_2\boldsymbol{v_2}\boldsymbol{v_2} + p_2\boldsymbol{I})) = p_I\nabla\alpha_2 + \alpha_2\rho_2 g \\ &\frac{\partial \alpha_2\rho_2 E_2}{\partial t} + \nabla \cdot \left(\alpha_2\boldsymbol{v_2}(\rho_2 E_2 + p_2)\right) = -p_I \frac{\partial}{\partial t}\alpha_2 \\ &\frac{\partial}{\partial t}\alpha_1 + \boldsymbol{v_I} \cdot \nabla\alpha_1 = 0 \end{aligned} \tag{2}$$

where α_j is the volume fraction of phase number j with the constraint $\alpha_1 + \alpha_2 = 1$, ρ_j is the fluid mass density, $\boldsymbol{v_j}$ the velocity vector, p_j is the pressure and $\rho_j E_j$ is the total energy per unit mass of phase number j, respectively. Furthermore, $\boldsymbol{g}$ is the vector of gravity acceleration. The model (2) must be closed by the equations of state for each phase that link the pressures p_j to the density and the internal energy and furthermore the model requires a proper choice of the

interface velocity $\boldsymbol{v_I}$ and the interface pressure p_I . Baer and Nunziato proposed the following choice

$$p_I = p_2, \text{ and } \boldsymbol{v_I} = \boldsymbol{v_1}, \qquad (3)$$

which we will also use in the present paper, since, as we show later, it is perfectly well suited for free–surface flow applications. We emphasize that model (2) is not written in conservative form. It contains the conservation equations of mass, momentum and energy for each phase, but the mutual interactions between the two phases are given by non–conservative terms on the right hand side. Furthermore, the volume fraction function α_1 is also governed by a convection equation written in non–conservative form. In this presentation viscous terms are not considered since the derived model is compared with the ideal Saint-Venant equations without friction. The discretization of viscous terms does not pose any particular difficulty and has been shown in [11] for the Navier-Stokes equations.

Simplified Three-Equation Model

The reduced model obtained in the next section is based on the following simplifications. The first assumption is that all pressures are relative pressures with respect to the atmospheric reference pressure $p_0=0$. Second, the gas surrounding the liquid is supposed to remain always at atmospheric reference conditions, i.e. the gas pressure is constant $p_2 = p_0 = 0$, which is a standard assumption for free surface flows in fluid mechanics. We therefore can neglect all evolution equations related to the gas phase $j = 2$ in the Baer–Nunziato model (2). Furthermore, according to the choice of Baer–Nunziato for the interface pressure given by eqn. (3), the interface pressure automatically results as $p_I = p_2 = p_0 = 0$. This is consistent with the usual standard assumption for free surface flows, where at the free surface of the liquid atmospheric reference pressure boundary conditions are imposed. Also the choice of the interface velocity $\boldsymbol{v_I} = \boldsymbol{v_I}$ according to (3) is consistent, since the interface will obviously propagate with the speed of the liquid phase. Third, the pressure of the liquid is computed by the Tait equation of state, see eqn. (4) below, which is in good agreement with the real behaviour of water in typical environmental flow conditions, i.e. close to atmospheric pressure and typical ambient temperatures. This equation of state is also very commonly used in weakly compressible smooth particle hydrodynamics (SPH) schemes for the simulation of free surface flows, see e.g. [4,5]. The key idea in the particular formulation of the Tait equation of state (EOS) is that according to the first assumption it yields a relative pressure with respect to the atmospheric reference pressure ($p_0 = 0$). We therefore have

$$p_1 = k_0 \left(\left(\frac{\rho_1}{\rho_0} \right)^{\gamma} - 1 \right) \qquad (4)$$

where k_0 is a constant that governs the compressibility of the fluid and hence the speed of sound, ρ_1 is the liquid density, ρ_0 is the liquid reference density at atmospheric standard conditions and γ is a parameter that is used to fit the EOS with experimental data. Since the EOS (4) does not depend explicitly on the internal energy, also the liquid energy equation in (2) can be dropped.

With the above simplifications, the final reduced three–equation model for free surface flows reads as follows:

$$\begin{aligned} \frac{\partial \alpha\rho}{\partial t} + \nabla \cdot (\alpha\rho\boldsymbol{v}) &= 0 \\ \frac{\partial \alpha\rho\boldsymbol{v}}{\partial t} + \nabla \cdot (\alpha(\rho\boldsymbol{v}\boldsymbol{v} + p\boldsymbol{I})) &= \alpha\rho g \\ \frac{\partial}{\partial t}\alpha + \boldsymbol{v} \cdot \nabla\alpha &= 0 \end{aligned} \qquad (5)$$

The above system can shown to be hyperbolic and the first two equations are written also in conservation form, i.e. the model conserves total mass and momentum.

Computational Results

The numerical method is based on the framework of $P_N P_M$ schemes of Dumbser et al. and has been described in great detail in [1,3,6]. Here, we present some computational examples to show the ability of the proposed model. For the numerical flux at the interface we use an Osher-type scheme [2], which in the conservative case [10] reads

$$\boldsymbol{f}_{i+\frac{1}{2}} = \frac{1}{2}(\boldsymbol{f}_i + \boldsymbol{f}_{i+1}) - \frac{1}{2}\int_0^1 |\boldsymbol{A}(\boldsymbol{\psi}(s))| ds \, (\boldsymbol{Q}_{i+1} - \boldsymbol{Q}_i) \qquad (6)$$

where Q is the vector of state, or the vector of conserved variables, f is the flux vector, A is the Jacobian of the flux f with respect to Q and $\psi(s)$ with $0 \le s \le 1$ is a straight-line segment path that connects the two states adjacent to the element-interface with each other in phase-space.

$$\boldsymbol{\psi}(s) = \boldsymbol{Q}_i + s(\boldsymbol{Q}_{i+1} - \boldsymbol{Q}_i) \qquad (7)$$

The integral in (6) is evaluated numerically using Gaussian quadrature formulae of appropriate accuracy.

A water jet impinging on an inclined plate

The test problem without gravity presented in this section consists of a water jet that impinges on a flat plate at an angle of $\alpha = 30$ degrees. The computational domain Ω can be seen in Fig. 1. The jet has a thickness of $H = 1$ and the initial density is set to $\rho = \rho_0$. The initial velocity is $\boldsymbol{v} = (5,0)$. In order to obtain a Mach number of $M = 0.3$ based on the known velocity, the constant k_0 is set to $k_0 = 2.78\text{E}5$. At the inclined wall we use reflective wall boundary conditions, at $x = 2$ in the interval $0 < y < 1$ we assume an

inflow boundary condition and all other boundaries are transmissive. The jet impinges on the wall and gets reflected asymmetrically due to the incidence angle h. After $t = 5$ a steady state is reached for the free surface. The results are depicted in Fig. 1, together with the exact solution given in [1].

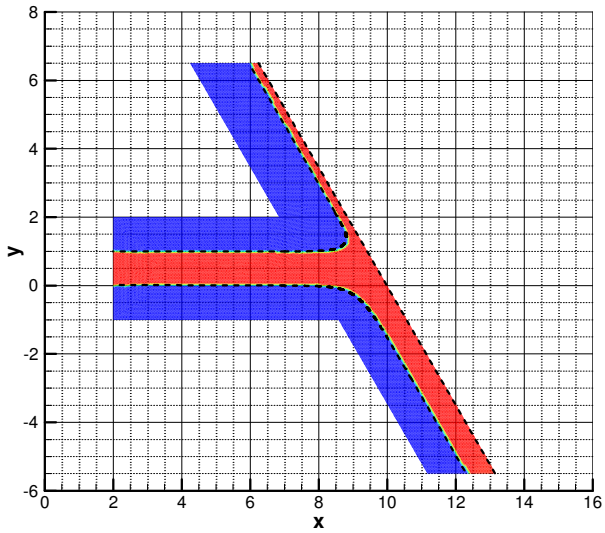

Figure 1: Exact (dashed line) and numerical solution (red area) for the jet impinging on the inclined flat plate.

Dambreak Problems

A very typical application for shallow water-type models is the so-called dambreak. It consists of the sudden collapse/removal of a vertical wall that separates two different piecewise constant states of water from each other. Since in the initial stages of dambreak flow, the classical shallow water assumption of small vertical velocities and accelerations does not hold, it is of interest to apply a more complete model to this well-studied phenomenon. In this section, we will compare the three-equation two-phase model against exact or numerical solutions of the shallow water equations. In particular, it is of great interest to compare the behaviour at small times (shortly after the dambreak) and at large times with each other. For a thorough study of the initial stages of three-dimensional dambreak flow see [6,7] together with a critical assessment of fully threedimensional hydrodynamic models and shallow water equations. For exact solutions of the dambreak problem in the shallow water context see [9] for the case with bottom step. For comparison purposes, we show together with the results of the new diffuse interface method also the free surface profile as computed by the SPH scheme of Ferrari et al. [6,7] using 224,282 SPH particles with a characteristic particle distance of $h = 0.03$. In all the test problems shown below, we can note an excellent agreement between the new two-phase flow model and the 2D SPH simulations, whereas there are

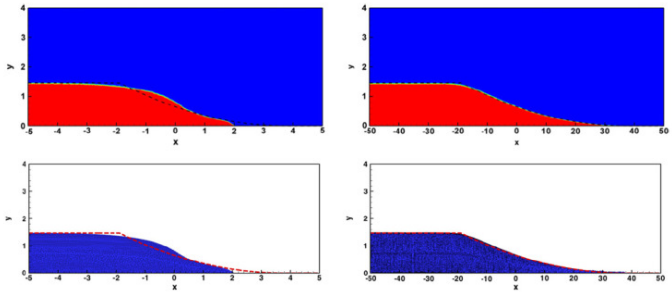

Figure 2: Shallow water solution (dashed line), multiphase method (red area in the top row) and SPH scheme (blue area in the bottom row) for a dambreak into dry bed.

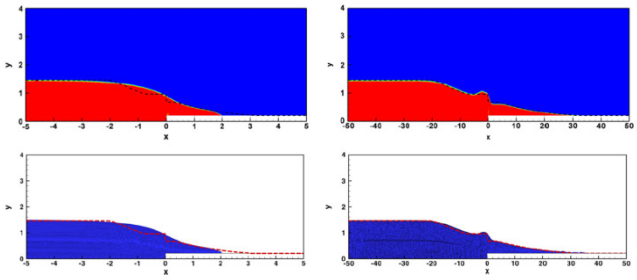

Figure 3: Shallow water solution (dashed line), multiphase method (red area in the top row) and SPH scheme (blue area in the bottom row) for a dambreak into dry bed with bottom step.

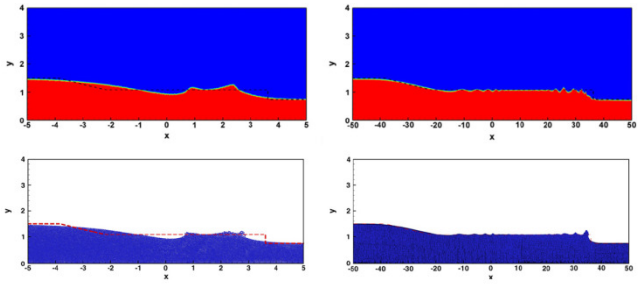

Figure 4: Shallow water solution (dashed line), multiphase method (red area in the top row) and SPH scheme (blue area in the bottom row) for a dambreak into wet bed.

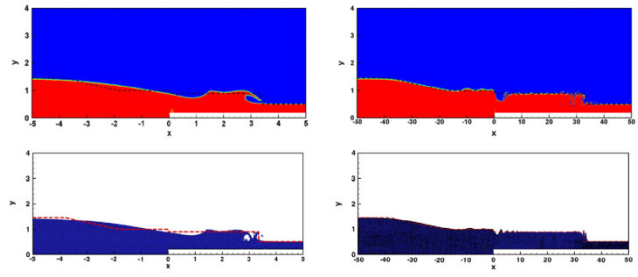

Figure 5: Shallow water solution (dashed line), multiphase method (red area in the top row) and SPH scheme (blue area in the bottom row) for a dambreak into wet bed with bottom step. Note the breaking waves on the free surface.

significant discrepancies between the full 2D models and the 1D shallow water model at short times. At large times, however, both weakly compressible 2D models agree very well with the shallow water theory, see Figures 2 and 3, respectively.

For the finite volume solution of the multi-phase flow model (3) we use a very fine mesh with 1,550,256 triangles of characteristic mesh spacing h = 0.01. The boundary conditions are reflective wall on the left, bottom and right border of the computational domain and transmissive boundaries on the top. The results obtained with the three-equation two-phase model at the early time t = 0.5 and at the late time t = 5.0 are presented in Figs. 2-5 and are compared against the exact solution of the shallow water equations [9]. We clearly see that at early times, the free surface profile predicted by the shallow water model does *not* agree with the two-phase model nor with the SPH solution. This is due to the fact that the shallow water model neglects vertical accelerations, which are very important in the initial phase of the dambreak. However, at large times (see Figs. 2-5 on the right), the shallow water assumptions are valid and hence a very good agreement between the shallow water solution and the solution obtained with the two-phase flow model and the SPH method is obtained. This result is particularly interesting because both solutions agree almost perfectly well despite the fact that two completely different models have been solved, namely in one case the one-dimensional version of the shallow water equations (1) and in the other case a three-equation two-phase flow model (3). However, since both PDE systems (1) and (3) are based on the first principles of conservation of mass and momentum, the overall wave propagation velocities are expected to be reproduced correctly by both physical models.

Flow over a sharp-crested weir

In this last section we study the flow over a sharp-crested weir. The setup of the test problem has been taken from [9]. The rectangular computational domain Ω = [0;15] x [0;2] contains an infinitely thin, sharp-crested weir of height h = 0.7 in the middle of the domain at x = 7.5, modeled as a reflective wall boundary. The initial domain containing liquid is Ω_l = [0; 7.5] x [0; 1.5], which leads to an overtopping of the water over the weir. The empirical formula for the lower streamline according to experiments of Scimemi is documented in [9] and which is shown in Figs. 6-7 as thick solid line. The density contour colours represent the numerical solution obtained by the three-equation two-phase flow model. We can note an excellent agreement between the numerical simulation and the experiments.

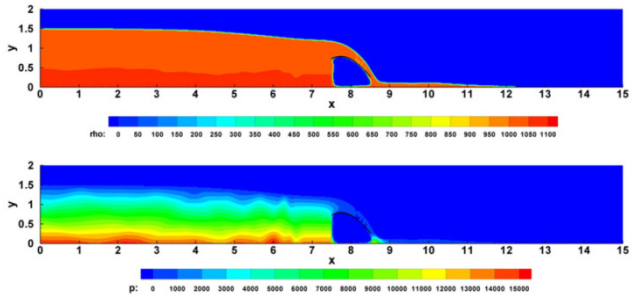

Figure 6: Flow over a sharp-crested weir at time t = 1.0. Density contours (top) and pressure contours (bottom) as obtained with the three-equation two-phase model. The experimental reference solution found by Scimemi and given in [9] is also shown (solid line).

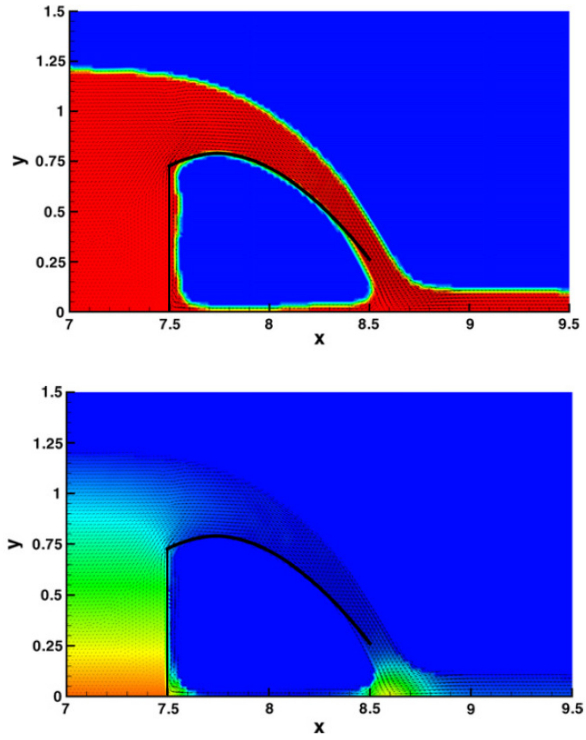

Figure 7: Zoom into the weir flow. Density contours (top) and pressure contours (bottom). The velocity vectors are also shown, together with the experimental profile found by Scimemi (solid line).

Conclusions

In this article it has been shown that free surface flows can also be accurately modeled using a *compressible* multi-phase flow model. The advantage over the usually incompressible volume of fluid (VOF) method is the fact that no elliptic pressure Poisson equation has to be solved and that hence all physical quantities can be directly evolved in time with an explicit scheme, which makes the method very simple and well suited for parallel implementation on modern supercomputers.

References

[1] M. Dumbser (2011). A simple two-phase method for the simulation of complex free surface flows, *Comput. Methods Appl. Mech. Engrg.* **200**: 1204–1219.

[2] M. Dumbser and E.F. Toro (2011). A Simple Extension of the Osher Riemann Solver to Non-Conservative Hyperbolic Systems. *Journal of Scientific Computing*, **48**:70-88.

[3] M. Dumbser, A. Hidalgo, M. Castro, C. Parés and E.F. Toro (2010). FORCE Schemes on Unstructured Meshes II: Non-Conservative Hyperbolic Systems. *Comput. Methods Appl. Mech. Engrg.*, **199**:625-647.

[4] M.R. Baer, J.W. Nunziato, (1986). A two-phase mixture theory for the deflagration-to-detonation transition (DDT) in reactive granular materials, J. Multiphase Flow **12**:861–889.

[5] M. Dumbser, D.S. Balsara, E.F. Toro and C.D. Munz (2008). A Unified Framework for the Construction of One-Step Finite-Volume and Discontinuous Galerkin Schemes on Unstructured Meshes, *Journal of Computational Physics*, **227**:8209–8253.

[6] A. Ferrari, M. Dumbser, E.F. Toro and A. Armanini (2009). A New 3D Parallel SPH scheme for Free Surface Flows. *Computers & Fluids*, **38**:1203-1217.

[7] A. Ferrari, L. Fraccarollo, M. Dumbser, E.F. Toro and A. Armanini (2010). Three-Dimensional Flow Evolution after a Dambreak. *Journal of Fluid Mechanics*, **663**:456-477.

[8] A. Ferrari (2010). SPH simulation of free surface flow over a sharp-crested weir, *Adv. Water Resour.* **33**:270–276.

[9] R. Bernetti, V.A. Titarev, E.F. Toro (2008). Exact solution of the Riemann problem for the shallow water equations with discontinuous bottom geometry, J. Comput. Phys. **227**:3212–3243.

[10] M. Dumbser and E.F. Toro (2011). On Universal Osher-Type Schemes for General Nonlinear Hyperbolic Conservation Laws. *Communications in Computational Physics*, **10**:635-671**.**

[11] M. Dumbser (2010). Arbitrary high order PNPM schemes on unstructured meshes for the compressible Navier–Stokes equations, *Computers & Fluids.* **39**:60–76.